
The continuous categorical: a novel simplex-valued exponential family

Elliott Gordon-Rodriguez¹ Gabriel Loaiza-Ganem² John P. Cunningham¹

Abstract

Simplex-valued data appear throughout statistics and machine learning, for example in the context of transfer learning and compression of deep networks. Existing models for this class of data rely on the Dirichlet distribution or other related loss functions; here we show these standard choices suffer systematically from a number of limitations, including bias and numerical issues that frustrate the use of flexible network models upstream of these distributions. We resolve these limitations by introducing a novel exponential family of distributions for modeling simplex-valued data – the *continuous categorical*, which arises as a nontrivial multivariate generalization of the recently discovered continuous Bernoulli. Unlike the Dirichlet and other typical choices, the continuous categorical results in a well-behaved probabilistic loss function that produces unbiased estimators, while preserving the mathematical simplicity of the Dirichlet. As well as exploring its theoretical properties, we introduce sampling methods for this distribution that are amenable to the reparameterization trick, and evaluate their performance. Lastly, we demonstrate that the continuous categorical outperforms standard choices empirically, across a simulation study, an applied example on multi-party elections, and a neural network compression task.¹

1. Introduction

Simplex-valued data, commonly referred to as *compositional data* in the statistics literature, are of great practical relevance across the natural and social sciences (see Pawlowsky-Glahn & Egozcue (2006); Pawlowsky-Glahn

& Buccianti (2011); Pawlowsky-Glahn et al. (2015) for an overview). Prominent examples appear in highly cited work ranging from geology (Pawlowsky-Glahn & Olea, 2004; Buccianti et al., 2006), chemistry (Buccianti & Pawlowsky-Glahn, 2005), biotechnology (Ebuehi & Oyewole, 2007), nutrition (Earle et al., 1968), psychiatry (Gueorguieva et al., 2008), ecology (Douma & Weedon, 2019), environmental science (Filzmoser et al., 2009), materials science (Na et al., 2014), political science (Katz & King, 1999; Tomz et al., 2002), public policy (Breunig & Busemeyer, 2012), economics (Fry et al., 2000), and the list goes on. An application of particular interest in machine learning arises in the context of model compression, where the class probabilities outputted by a large model are used as ‘soft targets’ to train a small neural network (Bucilu et al., 2006; Ba & Caruana, 2014; Hinton et al., 2015), an idea used also in transfer learning (Tzeng et al., 2015; Parisotto et al., 2015).

The existing statistical models of compositional data come in three flavors. Firstly, there are models based on a Dirichlet likelihood, for example the *Dirichlet GLM* (Campbell & Mosimann, 1987; Hijazi, 2003; Hijazi & Jernigan, 2009) and *Dirichlet Component Analysis* (Wang et al., 2008; Masoudimansour & Bouguila, 2017). Secondly, there are also models based on applying classical statistical techniques to \mathbb{R}^K -valued transformations of simplex-valued data, notably via *Logratios* (Aitchison, 1982; 1994; 1999; Egozcue et al., 2003; Aitchison & Egozcue, 2005). Thirdly, the machine learning literature has proposed predictive models that forgo the use of a probabilistic objective altogether and optimize the categorical cross-entropy instead (Ba & Caruana, 2014; Hinton et al., 2015; Sadowski & Baldi, 2018). The first type of model, fundamentally, suffers from an ill-behaved loss function (amongst other drawbacks) (§2), which constrain the practitioner to using inflexible (linear) models with only a small number of predictors. The second approach typically results in complicated likelihoods, which are hard to analyze and do not form an exponential family, forgoing many of the attractive theoretical properties of the Dirichlet. The third approach suffers from ignoring normalizing constants, sacrificing the properties of maximum likelihood estimation (see Loaiza-Ganem & Cunningham (2019) for a more detailed discussion of the pitfalls).

In this work, we resolve the three limitations simultaneously by defining a novel exponential family supported on

¹Department of Statistics, Columbia University
²Layer 6 AI. Correspondence to: Elliott Gordon-Rodriguez <eg2912@columbia.edu>, Gabriel Loaiza-Ganem <gabriel@layer6.ai>, John P. Cunningham <jpc2181@columbia.edu>.

¹Our code is available at https://github.com/cunningham-lab/cb_and_cc

the simplex, the *continuous categorical* (CC) distribution. Our distribution arises naturally as a multivariate generalization of the recently discovered continuous Bernoulli (CB) distribution (Loaiza-Ganem & Cunningham, 2019), a $[0, 1]$ -supported exponential family motivated by Variational Autoencoders (Kingma & Welling, 2014), which showed empirical improvements over the Beta distribution for modeling data which lies close to the extrema of the unit interval.

Similarly, the CC will provide three crucial advantages over the Dirichlet and other competitors; it defines a coherent, well-behaved and computationally tractable log-likelihood (§3.1, 3.4), which does not blow up in the presence of zero-valued observations (§3.2), and which produces unbiased estimators (§3.3). Moreover, the CC model presents no added complexity relative to its competitors; it has one fewer parameter than the Dirichlet as well as a similar functional form and a normalizing constant that can be written in closed form using elementary functions alone (§3.4). The continuous categorical brings probabilistic machine learning to the analysis of compositional data, opening up avenues for future applied and theoretical research.

2. Background

Careful consideration of the Dirichlet clarifies its shortcomings and the need for the CC family. The Dirichlet distribution is parameterized by $\alpha \in \mathbb{R}_+^K$ and defined on the simplex $\mathbb{S}^{K-1} = \{\mathbf{x} \in \mathbb{R}_+^{K-1} : \sum_{i=1}^{K-1} x_i < 1\}$ by:

$$p(x_1, \dots, x_{K-1}; \alpha) = \frac{1}{B(\alpha)} \prod_{i=1}^K x_i^{\alpha_i - 1}, \quad (1)$$

where $B(\alpha)$ denotes the multivariate Beta function, and $x_K = 1 - x_1 - \dots - x_{K-1}$.²

This density function presents an attractive combination of mathematical simplicity, computational tractability, and the flexibility to model both interior modes and sparsity, as well as defining an exponential family of distributions that provides a multivariate generalization of the Beta distribution and a conjugate prior to the multinomial distribution. As such, the Dirichlet is by far the best known and most widely used probability distribution for modeling simplex-valued random variables (Ng et al., 2011). This includes both the latent variables of mixed membership models (Erosheva, 2002; Blei et al., 2003; Barnard et al., 2003), and the statistical modeling of compositional outcomes (Aitchison, 1982; Campbell & Mosimann, 1987; Hijazi, 2003; Wang et al., 2008). Our work focuses on the latter, with special attention to the setting where we aim to learn a (possibly nonlinear) regression function that models a simplex-valued response

²Note that the K th component does not form part of the argument; it is a deterministic function of the $(K - 1)$ -dimensional random variable \mathbf{x} .

in terms of a (possibly large) set of predictors. In this context, and in spite of its strengths, the Dirichlet distribution suffers from three fundamental limitations.

First, flexibility: while the ability to capture interior modes might seem intuitively appealing, in practice it thwarts the optimization of predictive models of compositional data (as we will demonstrate empirically in section §5.2). To illustrate why, consider fitting a Dirichlet distribution to a single observation lying inside the simplex. Maximizing the likelihood will lead to a point mass on the observed datapoint (as was also noted by Sadowski & Baldi (2018)); the log-likelihood will diverge, and so will the parameter estimate (tending to ∞ along the line that preserves the observed proportions). This example may seem degenerate; after all, any dataset that would warrant a probabilistic model had better contain more than a single observation, at which point no individual point can ‘pull’ the density onto itself. However, in the context of predictive modeling, observations *will* often present unique input-output pairs, particularly if we have continuous predictors, or a large number of categorical ones. Thus, any regression function that is sufficiently flexible, such as a deep network, or that takes a sufficiently large number of inputs, can result in a divergent log-likelihood, frustrating an optimizer’s effort to find a sensible estimator. This limitation has constrained Dirichlet-based predictive models to the space of linear functions (Campbell & Mosimann, 1987; Hijazi & Jernigan, 2009).

Second, tails: the Dirichlet density diverges or vanishes at the extrema for all but a set of measure zero values of α , so that the log-likelihood is undefined whenever an observation contains zeros (transformation-based alternatives, such as Logratios, suffer the same drawback). However, zeros are ubiquitous in real-world compositional data, a fact that has led to the development of numerous hacks, such as Palarea-Albaladejo & Martín-Fernández (2008); Scealy & Welsh (2011); Stewart & Field (2011); Hijazi et al. (2011); Tsagris & Stewart (2018), each of which carries its own tradeoffs.

Third, bias: an elementary result is that the MLE of an exponential family yields an unbiased estimator for its sufficient statistic. However, the sufficient statistic of the Dirichlet distribution is the logarithm of the data, so that by Jensen’s inequality, the MLE for the mean parameter, which is typically the object of interest, is biased. While the MLE is also asymptotically consistent, this is only the case in the unrealistic setting of a true Dirichlet data-generating process, as we will illustrate empirically in section §5.1.

3. The continuous categorical distribution

These three limitations motivate the introduction of a novel exponential family, the *continuous categorical* (CC), which

is defined on the closed simplex, $\text{cl}(\mathbb{S}^{K-1})$, by:

$$\mathbf{x} \sim \mathcal{CC}(\boldsymbol{\lambda}) \iff p(x_1, \dots, x_{K-1}; \boldsymbol{\lambda}) \propto \prod_{i=1}^K \lambda_i^{x_i}, \quad (2)$$

where, again, $x_K = 1 - x_1 - \dots - x_{K-1}$. Without loss of generality we restrict the parameter values $\{\boldsymbol{\lambda} \in \mathbb{R}_+^K : \sum_i \lambda_i = 1\}$; such a choice makes the model identifiable. The CC density looks much like the Dirichlet, except that we have switched the role of the parameter and the variable. However, this simple exchange results in a well-behaved log-likelihood that can no longer concentrate mass on single interior points (§3.1), nor diverge at the extrema (§3.2), and that produces unbiased estimators (§3.3).

3.1. Convexity and modes

Because the CC log-likelihood is linear in the data (equation 2), the density is necessarily convex. It follows that the modes of the CC are at the extrema; example density plots are shown in figure 1. In this sense, the CC is a less flexible family than the Dirichlet, as it cannot represent interior modes. In the context of fitting a probability distribution (possibly in a regression setting) to compositional outcomes, however, this choice prevents the CC from concentrating mass on single observations, a fundamental tradeoff with the Dirichlet distribution and other transformation-based competitors such as Aitchison (1982; 1994; 1999). The mode of the CC is the basis vector associated with the $\text{argmax}(\lambda_1, \dots, \lambda_K)$ index of the data, provided the maximizer is unique.

3.2. Concentration of mass

The CC exhibits very different concentration of mass at the extrema relative to the Dirichlet. The former is always finite and strictly positive, whereas the latter either diverges or vanishes for almost all parameter values, in other words:

$$\lim_{x_j \rightarrow 0} \log \frac{\mathcal{CC}(\mathbf{x}|\boldsymbol{\lambda})}{\text{Dirichlet}(\mathbf{x}|\boldsymbol{\alpha})} \rightarrow \begin{cases} \infty, & \text{if } \alpha_j > 1 \\ -\infty, & \text{if } \alpha_j < 1 \end{cases}. \quad (3)$$

The important distinction lies at the limit points; the CC is supported on the *closed* simplex, whereas the Dirichlet and its transformation-based alternatives are defined only on its interior. Thus, the CC log-likelihood can automatically model data with zeros, without requiring specialized techniques such as Palarea-Albaladejo & Martín-Fernández (2008); Sealy & Welsh (2011); Stewart & Field (2011); Tsagris & Stewart (2018); Hijazi et al. (2011), to name but a few. The sheer amount of published work dedicated to this long-standing issue should convince the reader that this property of the CC distribution provides a substantial advantage in an applied modeling context.

3.3. Exponential Family

The CC defines an exponential family of distributions; noting that by definition $x_K = 1 - x_1 - \dots - x_{K-1}$, we can rewrite equation 2:

$$p(\mathbf{x}; \boldsymbol{\lambda}) \propto \exp\left(\sum_{i=1}^{K-1} x_i \log \frac{\lambda_i}{\lambda_K}\right). \quad (4)$$

Letting $\eta_i = \log \frac{\lambda_i}{\lambda_K}$, so that $\lambda_i = \frac{\exp(\eta_i)}{\sum_{k=1}^K \exp(\eta_k)}$, gives the natural parameter of our exponential family. Under this parameterization, we can ignore the K th component, $\eta_K = \log \frac{\lambda_K}{\lambda_K} \equiv 0$, and our parameter space becomes the unrestricted $\boldsymbol{\eta} \in \mathbb{R}^{K-1}$, which is much more convenient for optimization purposes and will be used throughout our implementation. With a slight abuse of notation,³ our density simplifies to:

$$p(x_1, \dots, x_{K-1}; \boldsymbol{\eta}) \propto \exp(\boldsymbol{\eta}^\top \mathbf{x}). \quad (5)$$

This last formulation makes it apparent that, under a CC likelihood, the mean of the data is minimal sufficient. By standard theory of exponential families, this implies that the MLE of the CC distribution will produce an unbiased estimator of the mean parameter. To be precise, if $\hat{\boldsymbol{\lambda}}$ maximizes the CC likelihood, and $\hat{\boldsymbol{\mu}}$ is the corresponding mean parameter obtained from $\hat{\boldsymbol{\lambda}}$, then $\hat{\boldsymbol{\mu}} = \bar{\mathbf{x}}$, where $\bar{\mathbf{x}}$ is the empirical average of the data. Thus, the CC MLE is unbiased for the true mean irrespective of the data-generating distribution.

This fact stands in contrast to the Dirichlet, in which the sufficient statistic is the mean of the logarithms, or other competitors, in which less can be said about the bias, partly as a result of their added complexities. Not only are these biases undesirable at a philosophical level, but we will also find in section 5 that, empirically, they compromise the performance of the Dirichlet relative to the CC.

3.4. Normalizing constant

For our new distribution to be of practical use, we must first derive its normalizing constant, which we denote by $C(\boldsymbol{\eta})$, defined by the equation:

$$\int_{\mathbb{S}^{K-1}} C(\boldsymbol{\eta}) \exp(\boldsymbol{\eta}^\top \mathbf{x}) d\mu = 1, \quad (6)$$

where μ is the Lebesgue measure.

Proposition. Let $S_K = \{1, 2, \dots, K\}$. The normalizing

³We will write $\mathbf{x} \sim \mathcal{CC}(\boldsymbol{\lambda})$ and $\mathbf{x} \sim \mathcal{CC}(\boldsymbol{\eta})$ interchangeably depending on context, and similarly with the density functions $p(\mathbf{x}; \boldsymbol{\lambda})$ and $p(\mathbf{x}; \boldsymbol{\eta})$.

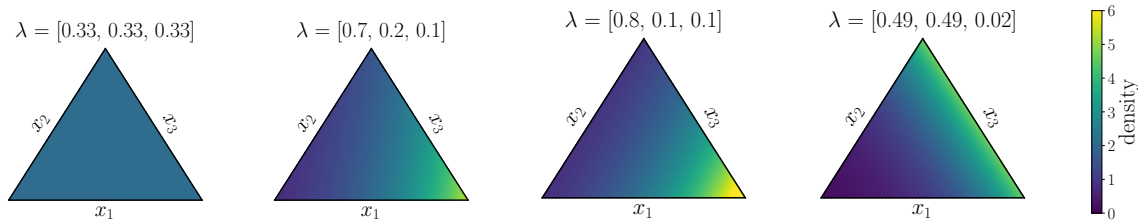


Figure 1. Density heatmaps of the 2-dimensional CC (defined on the 3-simplex). We show a near-uniform example, followed by more extremal examples, as well as a bimodal example (with the modes necessarily at the extrema). Note that, while we have defined the CC distribution on the space $\{\mathbf{x} : \sum_{i=1}^{K-1} x_i \leq 1\}$, we plot the density on the equivalent set $\{\mathbf{x} : \sum_{i=1}^K x_i = 1\}$.

constant of a $\mathcal{CC}(\boldsymbol{\eta})$ random variable is given by:

$$C(\boldsymbol{\eta}) = \frac{\prod_{i < j: i, j \in S_K} (\eta_i - \eta_j)}{\sum_{k=1}^K (-1)^{k+1} e^{\eta_k} \prod_{i < j: i, j \in S_K \setminus \{k\}} (\eta_i - \eta_j)}. \quad (7)$$

provided the denominator is not equal to zero.

Proof. We present a proof by induction in section A of the supplementary material.

It is worth noting that the denominator is equal to zero only on a set of Lebesgue measure zero, and while the CC is still properly defined in these cases, the normalizing constant takes a different form. Evaluating equation 7 when the denominator is close to zero can result in numerical instabilities. In our experiments (§5), the rare instances of this issue were dealt with by zeroing out any error-inducing gradients during optimization.

As shown in equation 7, the normalizing constant of the CC distribution exists in closed form as a composition of simple functions, whereas its Dirichlet counterpart is a product of Gamma functions. Therefore, the CC likelihood can be optimized straightforwardly using automatic differentiation, while the Dirichlet calls for specialized numerical techniques (Ronning, 1989; Minka, 2000). Thus, it is worth emphasizing that not only is the CC distribution able to address several key limitations of the Dirichlet, but it also does so without sacrificing mathematical simplicity (the form of the densities are very similar) or exponential family properties, or adding additional parameters.

3.5. Mean and variance

By the standard theory of exponential families, the mean and covariance of the CC distribution can be computed by differentiating the normalizing constant. Thus, while cumbersome to write down analytically, we can evaluate these quantities using automatic differentiation. Higher moments, including skewness and kurtosis, can also be derived from the normalizing constant, as well as a number of other dis-

tributonal results, such as the characteristic function or KL divergence (see section B from the supplementary material).

3.6. Related distributions

The Dirichlet distribution can be thought of as a natural generalization of the Beta distribution to higher dimensions, which arises by taking the product of independent Beta densities and restricting the resulting function to the simplex. In the same way, the CC provides a multivariate extension of the recently proposed continuous Bernoulli (CB) distribution (Loaiza-Ganem & Cunningham, 2019), which is defined on $[0, 1]$ by:

$$x \sim \mathcal{CB}(\lambda) \iff p(x|\lambda) \propto \lambda^x (1-\lambda)^{1-x}. \quad (8)$$

First, observe that this density is equivalent to the univariate case of the CC (i.e. $K = 2$). Second, note that the full CC density (2) corresponds to the product of independent CB densities, restricted to the simplex, an idea that we will capitalize on when designing sampling algorithms for the CC (§4). In this sense, the Beta, Dirichlet, CB and CC distributions form an intimately connected tetrad; the CB and the CC switch the role of the parameter and the variable in the Beta and Dirichlet densities, respectively, and the Dirichlet and CC extend to the simplex the product of Beta and CB densities, respectively. The analogy to the Beta and CB families is not just theoretical; the CB arose in the context of Variational Autoencoders (Kingma & Welling, 2014) and showed empirical improvements over the Beta for modeling data which lies close to the extrema of the unit interval (Loaiza-Ganem & Cunningham, 2019). Similarly, the CC provides theoretical and empirical improvements over the Dirichlet for modeling extremal data (§3.2, 5).

4. Sampling

Sampling is of fundamental importance for any probability distribution. We developed two novel sampling schemes for the CC, which we highlight here; full derivations and a study of their performance (including reparameterization

gradients) can be found in the supplement (section C).

First, given the relationship between the CB and the CC densities (§3.6), a naive rejection sampler for the CC follows directly by combining independent CB draws (using the closed form inverse cdf), and accepting only draws on the simplex. This basic sampler scales poorly in K . We improve upon it via a reordering operation, which has vastly better performance both empirically and theoretically (see section CC). The central concept of this scheme is to sort the parameter λ and reject as soon as samples leave the simplex; this sampler is shown in algorithm 1.

Algorithm 1 Ordered rejection sampler

Input: target distribution $\mathcal{CC}(\lambda)$.

Output: sample \mathbf{x} drawn from target.

- 1: Find the sorting operator π that orders λ from largest to smallest, and let $\tilde{\lambda} = \pi(\lambda)$.
 - 2: Set the cumulative sum $c \leftarrow 0$ and $i \leftarrow 2$.
 - 3: **while** $c < 1$ and $i \leq K$ **do**
 - 4: Sample $x_i \sim \mathcal{CB}\left(\tilde{\lambda}_i / (\tilde{\lambda}_i + \tilde{\lambda}_1)\right)$.
 - 5: Set $c \leftarrow c + x_i$ and
 - 6: Set $i \leftarrow i + 1$.
 - 7: **end while**
 - 8: If $c > 1$, go back to step 2.
 - 9: Set $x_1 = 1 - \sum_{i=2}^K x_i$.
 - 10: Return $\mathbf{x} = \pi^{-1}(x_1, \dots, x_K)$.
-

Algorithm 1 performs particularly well in the case that λ is unbalanced, with a small number of components concentrating most of the mass (see figure 1 in the supplement). However, its efficiency degrades under balanced configurations of λ ; this shortcoming motivates the need for our second sampler (algorithm 2), which performs particularly well in the balanced setting. Conceptually, this second sampler will exploit a permutation-induced partition of the unit cube into simplices, combined with a relaxation of the CC which is invariant under permutations, and can be mapped back to the original CC distribution.

At a technical level, first note that if σ is a permutation of $\{1, \dots, K-1\}$ and $\mathcal{S}_\sigma = \{\mathbf{x} \in \mathbb{R}^{K-1} : 0 \leq x_{\sigma(1)} \leq x_{\sigma(2)} \leq \dots \leq x_{\sigma(K-1)} \leq 1\}$, then we can (almost, in the measure-theoretic sense) partition $[0, 1]^{K-1} = \bigcup \mathcal{S}_\sigma$ where the union is over all permutations. Second, we can generalize the CC to an arbitrary sample space by writing $p_\Omega(\mathbf{x}|\eta) \propto \exp(\eta^\top \mathbf{x}) \mathbb{1}(\mathbf{x} \in \Omega)$. We note that this family is invariant to invertible linear maps in the sense that, if $\mathbf{x} \sim p_{\mathcal{A}}(\mathbf{x}|\eta)$ and $\mathbf{y} = Q\mathbf{x}$, where Q is an invertible matrix, then $\mathbf{y} \sim p_{Q(\mathcal{A})}(\mathbf{y}|\tilde{\eta})$, where $\tilde{\eta} = Q^{-\top}\eta$. Putting these two facts together, if B is a lower-triangular matrix of ones and id denotes the identity permutation, then $\mathcal{S}_{id} = B(\text{cl}(\mathbb{S}^{K-1}))$, and it follows that we can sample from $\mathbf{x} \sim \mathcal{CC}(\eta)$ by sampling $\mathbf{y} \sim p_{\mathcal{S}_{id}}(\mathbf{y}|\tilde{\eta})$ and trans-

forming with $\mathbf{x} = B^{-1}\mathbf{y}$. Conveniently, $p_{\mathcal{S}_{id}}(\cdot|\tilde{\eta})$ can be sampled efficiently by drawing a $[0, 1]^{K-1}$ -valued vector of independent CB variates, transforming into \mathcal{S}_{id} by applying a suitable permutation matrix P , and accepting with the appropriate probability. This scheme is shown altogether in algorithm 2: we rejection sample using the transformed sample as the proposal, where the rejection sampling constant will depend on the permutation matrix P (see equation 23 from the supplementary material).

Algorithm 2 Permutation sampler

Input: target distribution $\mathcal{CC}(\eta)$.

Output: sample \mathbf{x} drawn from target.

- 1: Sample $\mathbf{y} \sim p_{[0,1]^{K-1}}(\cdot|\tilde{\eta})$, where $\tilde{\eta} = B^{-\top}\eta$.
 - 2: Let $\mathbf{y}' = P\mathbf{y}$, where P is the permutation matrix that sorts \mathbf{y} in increasing order.
 - 3: Accept \mathbf{y}' with an appropriate probability. Otherwise, go back to step 2.
 - 4: Return $\mathbf{x} = B^{-1}\mathbf{y}'$.
-

This permutation sampler performs particularly well in the case that λ is balanced, which, taken together with algorithm 1, provides an efficient, theoretically understood, and reparameterizable sampling scheme for the CC.

5. Experiments

5.1. Simulation study

We begin our experiments with a simulation study that illustrates the biases incurred from fitting Dirichlet distributions to compositional data. Our procedure is as follows:

1. Fix a ground-truth distribution $\mathbf{x} \sim p(\mathbf{x})$ on the simplex. This will either be a Dirichlet where the (known) parameter value α is drawn from independent $\text{Exp}(1)$ variates, or a CC where the (known) parameter value λ is sampled uniformly on the simplex.
2. Fix a sample size n . This will range from $n = 2$ to $n = 20$.
3. In each of one million trials, draw a sample of n i.i.d. observations $\mathbf{x}_i \sim p(\mathbf{x})$.
4. Use the samples to compute one million MLEs of the mean parameter, under both a Dirichlet and a CC likelihood.
5. Average the MLEs over the million trials to obtain the ‘empirical mean’, and subtract the true mean $\mathbb{E}_{p(\mathbf{x})}[\mathbf{x}]$ to obtain estimates of the ‘empirical bias’.
6. Repeat the steps for different values of α , λ , and n , as prescribed.

The results of this experiment are shown in figure 2. As we already knew from the theory of exponential families, only

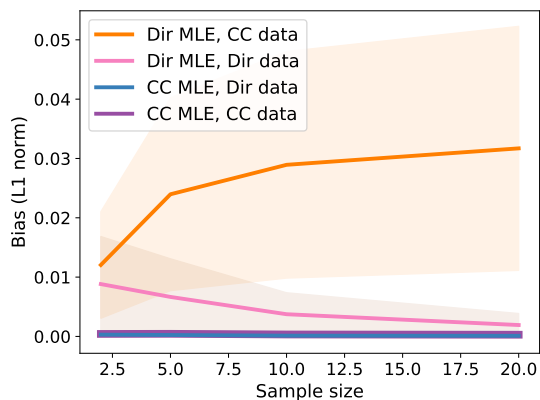


Figure 2. Empirical bias of the Dirichlet and CC MLEs as a function of sample size, for $K = 3$ (other values of K behaved similarly). The error bars show ± 1 standard deviation over different draws of the parameters of the ground-truth model from their respective priors. Regardless of whether the synthetic data is generated from a Dirichlet or a CC, only the CC estimator is unbiased.

the CC estimator is unbiased. The Dirichlet estimator is, at best, asymptotically unbiased, and only in the unrealistic setting of a true Dirichlet generative process (pink line). It is worth emphasizing that, even in this most-favorable case for the Dirichlet, the CC outperforms (pink line versus blue line). The error bars show ± 1 standard deviation over different draws from the prior distribution of step 1. The large error bars on the Dirichlet, especially under non-Dirichlet data (orange line) indicate that its bias is highly sensitive the true mean of the distribution, reaching up to several percentage points, whereas the CC is unbiased across the board. Lastly, note that while a sample size of 20 may seem small in a machine learning context, this is in fact reasonable in terms of the ratio of observations to parameters, as larger samples typically call for more flexible models.

5.2. UK election data

We next consider a real-world example from the 2019 UK general election (Uberoi et al., 2019). The UK electorate is divided into 650 constituencies, each of which elects 1 member of parliament (MP) in a winner-takes-all vote. Typically, each of the major parties will be represented in each constituency, and will win a share of that constituency’s electorate. Thus, our data consists of 650 observations⁴, each of which is a vector of proportions over the four major parties (plus a fifth proportion for a ‘remainder’ category, which groups together smaller parties and independent candidates). We regress this outcome on four predictors: the region of the constituency (a categorical variable with 4 levels), an ur-

⁴We split the data into an 80/20 training and test set at random.

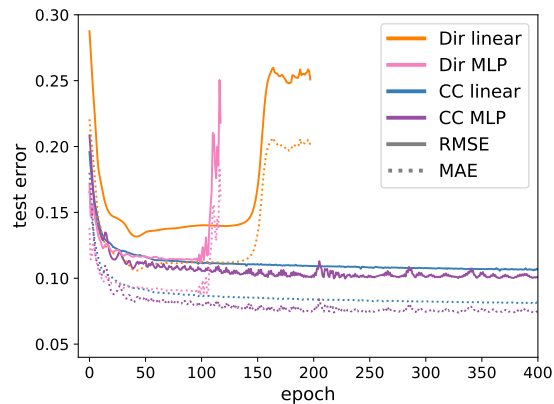


Figure 3. Test error for the linear and MLP models with a Dirichlet and CC log-likelihood. The CC objective is better-behaved, training more smoothly and converging to the MLE, unlike the Dirichlet log-likelihood which diverges, causing overfitting.

ban/rural indicator, the size of the constituency’s electorate, and the voter turnout percentage from the previous general election. While there is a host of demographic data that could be used to construct increasingly more informative predictors here, we stick to the reduced number of variables that were available in our original dataset, as the goal of our analysis is *not* to build a strong predictive model, but rather to illustrate the advantages and disadvantages of using the novel CC distribution as opposed to the Dirichlet. For the benefit of the latter, since our data contains zeros (not all major parties are represented in all constituencies), we add an insignificant 0.1% share to all observations and re-normalize prior to modeling (without this data distortion, the Dirichlet would fail even more grievously).

We fit regression networks to this data with two different loss functions, one where we assume the response follows a Dirichlet likelihood (Campbell & Mosimann, 1987; Hijazi, 2003; Hijazi & Jernigan, 2009), the other with our own CC likelihood instead. We first fit the simplest linear version: for the Dirichlet, we map the inputs into the space of α by applying a single linear transformation followed by an exp activation function; for the CC, a single linear transformation is sufficient to map the inputs to the unconstrained space of η (in statistical terms, this corresponds to a generalized linear model with canonical link). Secondly, we extend our linear model to a more flexible neural network by adding a hidden layer with 20 units and ReLU activations. We train both models using Adam (Kingma & Ba, 2015).

The CC models achieve better test error; the gain is around 10–30% in the L_1 and L_2 sense, as shown in table 1 and figure 3.⁵ Moreover, the CC reliably converges to a performant

⁵The L_1 and L_2 metrics are used for illustration purposes. One

Table 1. Test errors for our regression models of the UK election data. Both in the linear and MLP case, the CC model beats the Dirichlet counterpart.

	MAE	RMSE
DIR LINEAR	0.105	0.132
CC LINEAR	0.075	0.101
DIR MLP	0.087	0.112
CC MLP	0.072	0.097

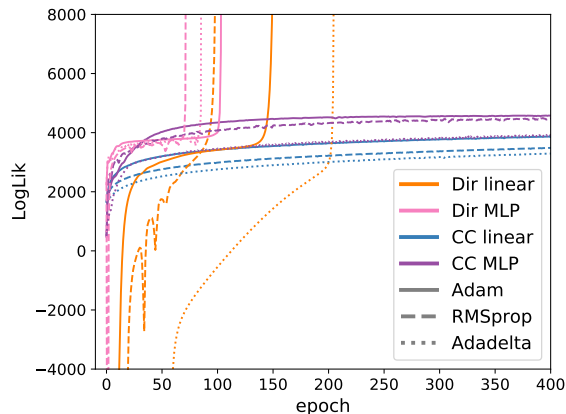


Figure 4. Log-likelihood during training with different optimizers for the Dirichlet and the CC models. Consistently across optimizers, the CC objective converges to the MLE and the Dirichlet diverges.

model (which in the linear case corresponds to the MLE), whereas the Dirichlet likelihood diverges along a highly variable path in the parameter space that correspond to sub-optimal models. We verify also that this behavior happens irrespective of the optimizer used to train the model (figure 4), and is consistent across random initializations of the model parameters (figure 5). Note that the Dirichlet MLP diverges faster than its linear counterpart, likely because the increased flexibility afforded by the MLP architecture allows it to place a spike on a training point more quickly.

Naturally, one might ask whether the unstable behavior of the Dirichlet can be fixed through regularization, as a suitable penalty term might be able to counterbalance the detrimental flexibility of the distribution. We test this hypothesis empirically by adding an L_2 penalty (in the space of the natural parameter) to the objective, with a varying coefficient to control the regularization strength. The results are shown in figure 6; while strong regularization does stabilize the Dirichlet, it is still unable to outperform the

could, of course, optimize these metrics directly, however this would either jeopardize the probabilistic interpretation and statistical rigor of the model, or require the addition of an intractable normalizing constant to the log-likelihood.

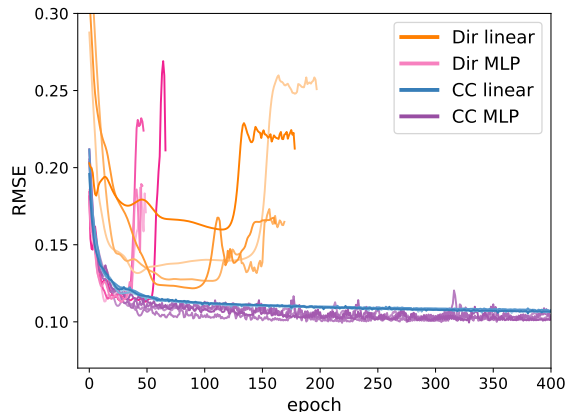


Figure 5. Test error for different random initializations of the model parameters. The CC model converges, whereas the Dirichlet diverges along a highly variable path in the parameter space, and the models it finds in this path are suboptimal.

(unregularized) CC and it is slower to converge.

5.3. Model compression

Our last experiment considers a typical model compression task (Bucilu et al., 2006; Ba & Caruana, 2014; Hinton et al., 2015), where we have access to an accurate ‘teacher’ model that is expensive to evaluate, which we use in order to train a cheaper ‘student’ model, typically a neural network with few layers. By training the student network to predict the fitted values of the teacher model, it can achieve better generalization than when trained on the original labels, as was shown by Bucilu et al. (2006); Ba & Caruana (2014); Hinton et al. (2015). These fitted values provide ‘soft targets’ that are typically located close to the extrema of the simplex, though we can also bring them towards the centroid while conserving their relative order by varying the temperature, T , of the final softmax (Hinton et al., 2015).

We build on the MNIST experiment of Hinton et al. (2015); we first train a teacher neural net with two hidden layers of 1200 units and ReLU activations, regularized using batch normalization, and we use its fitted values to train smaller student networks with a single hidden layer of 30 units. We fit the student networks to the soft targets using the categorical cross-entropy (XE) loss, as well as a Dirichlet (as per Sadowski & Baldi (2018)) and a CC log-likelihood. The latter is equivalent to adding the appropriate normalization constant to the XE, thus giving a correct probabilistic interpretation to the procedure. Moreover, the XE and the CC objective result in the same estimator at optimality: the empirical mean of the data (we know this is true theoretically from section 3.3). However, the two objectives define different optimization landscapes, so the question of which

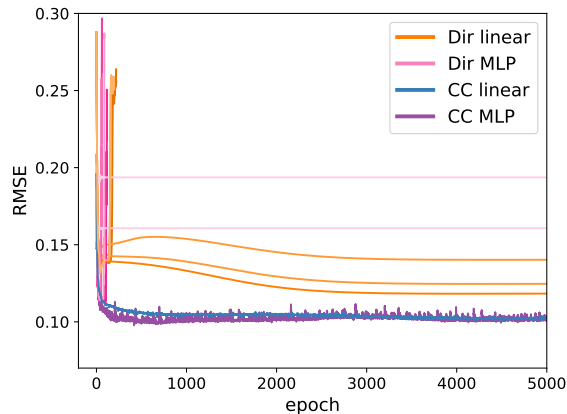


Figure 6. Test error for different regularization strengths for the Dirichlet models. Lighter shades of pink and orange indicate increasing regularization strengths. While sufficiently strong regularization does stabilize the Dirichlet, preventing it from diverging, it still does not outperform the (unregularized) CC.

Table 2. Test errors for the student models trained under the Dirichlet, XE, and CC objectives, as well as using the hard labels instead of the teacher model. We show the best values obtained over over 5 random initializations and the 3 temperature settings of figure 7.

OBJECTIVE	MISCLASSIFICATION RATE	RMSE
DIRICHLET	9.4%	0.041
SOFT XE	5.4%	0.029
CC	4.4%	0.024
HARD XE	6.8%	—

one to use becomes an empirical one.

In this case, we found that using the CC objective leads to a lower misclassification rate on the test set than the XE (table 2), as well as a lower RMSE (measured against the soft targets outputted by the trained teacher model when evaluated on the test set), and did so consistently across temperatures (figure 7). Both the CC and XE objectives worked substantially better than the Dirichlet likelihood, and better than training the same architecture on the original hard labels. Note also that the Dirichlet performs very poorly and is unstable in the unadjusted temperature setting ($T = 1$), as the soft targets are very extremal and lead to numerical overflow, but performs much better at high temperatures.

5.4. Mixed membership models

While we have shown that the CC provides empirical improvements in predictive models of compositional data, it is also worth noting that we do not expect this distribution to perform on par with the Dirichlet and other competitors in the context of mixed membership models, such as Pritchard

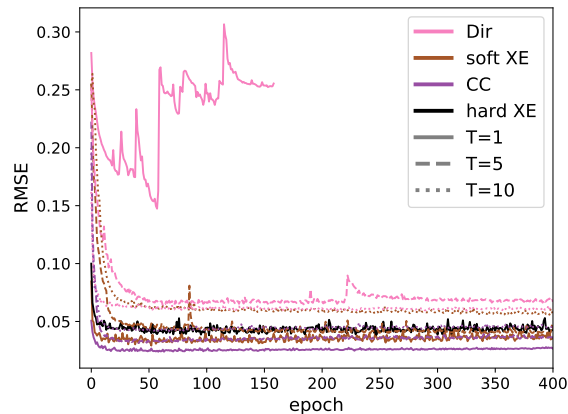


Figure 7. Test error at different temperatures for the Dirichlet, XE and CC objectives. For each student model, this error measures the L_2 difference between its fitted values and those of the teacher model, on the test set.

et al. (2000); Erosheva (2002); Blei et al. (2003); Barnard et al. (2003). For example, using the CC to model class-membership in the latent space of a VAE resulted in poor results, partly due to the CC not being sufficiently flexible to approximate a categorical distribution, unlike other continuous relaxations that have been proposed in the literature, such as Jang et al. (2016); Maddison et al. (2016).

6. Conclusion

Our results demonstrate the theoretical and empirical benefits of the CC, which should hold across a range of applied modeling contexts. To conclude, we summarize the main contributions of our work:

- We have introduced the CC distribution, a novel exponential family defined on the simplex, that resolves a number of long-standing limitations of previous models of compositional data.
- We have fully characterized our distribution and discussed its theoretical properties. Of particular importance is the sufficient statistic, which guarantees unbiased estimators, and the favorable behavior of the log-likelihood, which leads to ease of optimization and robustness to extreme values.
- Empirically, the CC defines probabilistic models that outperform their Dirichlet counterparts and other competitors, and allows for a rich class of regression functions, including neural networks.
- We have also designed and implemented novel and efficient rejection sampling algorithms for the CC.

Taken together, these findings indicate the CC is a valuable

density for probabilistic machine learning with simplex-valued data.

References

- Aitchison, J. The statistical analysis of compositional data. *Journal of the Royal Statistical Society: Series B (Methodological)*, 44(2):139–160, 1982.
- Aitchison, J. Principles of compositional data analysis. *Lecture Notes-Monograph Series*, 24:73–81, 1994. ISSN 07492170.
- Aitchison, J. Logratios and natural laws in compositional data analysis. *Mathematical Geology*, 31(5):563–580, 1999.
- Aitchison, J. and Egozcue, J. J. Compositional data analysis: where are we and where should we be heading? *Mathematical Geology*, 37(7):829–850, 2005.
- Ba, J. and Caruana, R. Do deep nets really need to be deep? In *Advances in neural information processing systems*, pp. 2654–2662, 2014.
- Barnard, K., Duygulu, P., Forsyth, D., Freitas, N. d., Blei, D. M., and Jordan, M. I. Matching words and pictures. *Journal of machine learning research*, 3(Feb):1107–1135, 2003.
- Blei, D. M., Ng, A. Y., and Jordan, M. I. Latent dirichlet allocation. *Journal of machine Learning research*, 3(Jan): 993–1022, 2003.
- Breunig, C. and Busemeyer, M. R. Fiscal austerity and the trade-off between public investment and social spending. *Journal of European Public Policy*, 19(6):921–938, 2012.
- Buccianti, A. and Pawlowsky-Glahn, V. New perspectives on water chemistry and compositional data analysis. *Mathematical Geology*, 37(7):703–727, 2005.
- Buccianti, A., Mateu-Figueras, G., and Pawlowsky-Glahn, V. Compositional data analysis in the geosciences: From theory to practice. Geological Society of London, 2006.
- Bucilu, C., Caruana, R., and Niculescu-Mizil, A. Model compression. In *Proceedings of the 12th ACM SIGKDD international conference on Knowledge discovery and data mining*, pp. 535–541, 2006.
- Campbell, G. and Mosimann, J. Multivariate methods for proportional shape. In *ASA Proceedings of the Section on Statistical Graphics*, volume 1, pp. 10–17. Washington, 1987.
- Douma, J. C. and Weedon, J. T. Analysing continuous proportions in ecology and evolution: A practical introduction to beta and dirichlet regression. *Methods in Ecology and Evolution*, 10(9):1412–1430, 2019.
- Earle, F., Vanetten, C., Clark, T., and Wolff, I. Compositional data on sunflower seed. *Journal of the American Oil Chemists’ Society*, 45(12):876–879, 1968.
- Ebuehi, O. A. T. and Oyewole, A. C. Effect of cooking and soaking on physical characteristics, nutrient composition and sensory evaluation of indigenous and foreign rice varieties in nigeria. *African Journal of Biotechnology*, 6 (8), 2007.
- Egozcue, J. J., Pawlowsky-Glahn, V., Mateu-Figueras, G., and Barcelo-Vidal, C. Isometric logratio transformations for compositional data analysis. *Mathematical Geology*, 35(3):279–300, 2003.
- Erosheva, E. A. *Grade of membership and latent structure models with application to disability survey data*. PhD thesis, PhD thesis, Carnegie Mellon University, Department of Statistics, 2002.
- Filzmoser, P., Hron, K., and Reimann, C. Univariate statistical analysis of environmental (compositional) data: problems and possibilities. *Science of the Total Environment*, 407(23):6100–6108, 2009.
- Fry, J. M., Fry, T. R., and McLaren, K. R. Compositional data analysis and zeros in micro data. *Applied Economics*, 32(8):953–959, 2000.
- Gamerman, D. and Lopes, H. F. *Markov chain Monte Carlo: stochastic simulation for Bayesian inference*. Chapman and Hall/CRC, 2006.
- Gueorguieva, R., Rosenheck, R., and Zelteman, D. Dirichlet component regression and its applications to psychiatric data. *Computational statistics & data analysis*, 52 (12):5344–5355, 2008.
- Hijazi, R. et al. An em-algorithm based method to deal with rounded zeros in compositional data under dirichlet models. 2011.
- Hijazi, R. H. *Analysis of compositional data using Dirichlet covariate models*. PhD thesis, American University, 2003.
- Hijazi, R. H. and Jernigan, R. W. Modelling compositional data using dirichlet regression models. *Journal of Applied Probability & Statistics*, 4(1):77–91, 2009.
- Hinton, G., Vinyals, O., and Dean, J. Distilling the knowledge in a neural network. In *NIPS Deep Learning and Representation Learning Workshop*, 2015.
- Jang, E., Gu, S., and Poole, B. Categorical reparameterization with gumbel-softmax. *arXiv preprint arXiv:1611.01144*, 2016.

- Katz, J. N. and King, G. A statistical model for multiparty electoral data. *American Political Science Review*, 93(1): 15–32, 1999.
- Kingma, D. P. and Ba, J. Adam: A method for stochastic optimization. In *3rd International Conference on Learning Representations, ICLR 2015, San Diego, CA, USA, May 7-9, 2015, Conference Track Proceedings*, 2015.
- Kingma, D. P. and Welling, M. Auto-encoding variational bayes. In *2nd International Conference on Learning Representations, ICLR 2014, Banff, AB, Canada, April 14-16, 2014, Conference Track Proceedings*, 2014.
- Loaiza-Ganem, G. and Cunningham, J. P. The continuous bernoulli: fixing a pervasive error in variational autoencoders. In *Advances in Neural Information Processing Systems*, pp. 13266–13276, 2019.
- Maddison, C. J., Mnih, A., and Teh, Y. W. The concrete distribution: A continuous relaxation of discrete random variables. *arXiv preprint arXiv:1611.00712*, 2016.
- Masoudimansour, W. and Bouguila, N. Dirichlet mixture matching projection for supervised linear dimensionality reduction of proportional data. In *2017 IEEE International Conference on Acoustics, Speech and Signal Processing (ICASSP)*, pp. 2806–2810. IEEE, 2017.
- Minka, T. Estimating a dirichlet distribution, 2000.
- Na, J. H., Demetriou, M. D., Floyd, M., Hoff, A., Garrett, G. R., and Johnson, W. L. Compositional landscape for glass formation in metal alloys. *Proceedings of the National Academy of Sciences*, 111(25):9031–9036, 2014.
- Ng, K. W., Tian, G.-L., and Tang, M.-L. *Dirichlet and related distributions: Theory, methods and applications*, volume 888. John Wiley & Sons, 2011.
- Palarea-Albaladejo, J. and Martín-Fernández, J. A modified em algorithm for replacing rounded zeros in compositional data sets. *Computers & Geosciences*, 34(8): 902–917, 2008.
- Parisotto, E., Ba, J. L., and Salakhutdinov, R. Actor-mimic: Deep multitask and transfer reinforcement learning. *arXiv preprint arXiv:1511.06342*, 2015.
- Pawlowsky-Glahn, V. and Buccianti, A. *Compositional data analysis*. Wiley Online Library, 2011.
- Pawlowsky-Glahn, V. and Egozcue, J. J. Compositional data and their analysis: an introduction. *Geological Society, London, Special Publications*, 264(1):1–10, 2006.
- Pawlowsky-Glahn, V. and Olea, R. A. *Geostatistical analysis of compositional data*, volume 7. Oxford University Press, 2004.
- Pawlowsky-Glahn, V., Egozcue, J. J., and Tolosana-Delgado, R. *Modeling and analysis of compositional data*. John Wiley & Sons, 2015.
- Pritchard, J. K., Stephens, M., and Donnelly, P. Inference of population structure using multilocus genotype data. *Genetics*, 155(2):945–959, 2000.
- Ronning, G. Maximum likelihood estimation of dirichlet distributions. *Journal of statistical computation and simulation*, 32(4):215–221, 1989.
- Sadowski, P. and Baldi, P. Neural network regression with beta, dirichlet, and dirichlet-multinomial outputs. 2018.
- Scealy, J. and Welsh, A. Regression for compositional data by using distributions defined on the hypersphere. *Journal of the Royal Statistical Society: Series B (Statistical Methodology)*, 73(3):351–375, 2011.
- Stewart, C. and Field, C. Managing the essential zeros in quantitative fatty acid signature analysis. *Journal of Agricultural, Biological, and Environmental Statistics*, 16(1):45–69, 2011.
- Tomz, M., Tucker, J. A., and Wittenberg, J. An easy and accurate regression model for multiparty electoral data. *Political Analysis*, 10(1):66–83, 2002.
- Tsagris, M. and Stewart, C. A dirichlet regression model for compositional data with zeros. *Lobachevskii Journal of Mathematics*, 39(3):398–412, 2018.
- Tzeng, E., Hoffman, J., Darrell, T., and Saenko, K. Simultaneous deep transfer across domains and tasks. In *Proceedings of the IEEE International Conference on Computer Vision*, pp. 4068–4076, 2015.
- Uberoi, E., Baker, C., and Cracknell, R. General election 2019: Full results and analysis. *Parliament UK*. July, 2019.
- Wang, H.-Y., Yang, Q., Qin, H., and Zha, H. Dirichlet component analysis: feature extraction for compositional data. In *Proceedings of the 25th international conference on Machine learning*, pp. 1128–1135. ACM, 2008.

Supplementary material for: The continuous categorical: a novel simplex-valued exponential family

A. Derivation of the normalizing constant

For clarity, we start by recalling the expression that we aim to show (equation 7 from the main text), and we make the dependence on K explicit by writing $C_K(\boldsymbol{\eta})$:

$$C_K(\boldsymbol{\eta}) = \frac{\prod_{i < j: i, j \in S_K} (\eta_i - \eta_j)}{\sum_{k=1}^K (-1)^{k+1} e^{\eta_k} \prod_{i < j: i, j \in S_K \setminus \{k\}} (\eta_i - \eta_j)}, \quad (1)$$

or equivalently, taking the inverse:

$$C_K(\boldsymbol{\eta})^{-1} = (-1)^{K+1} \sum_{k=1}^K \frac{\exp(\eta_k)}{\prod_{i \neq k} (\eta_i - \eta_k)}. \quad (2)$$

Proof: we proceed by induction on K . We assume that equation 2 gives the correct normalizing constant for $K - 1$, and compute the integral for K :

$$\begin{aligned} C_K(\boldsymbol{\eta})^{-1} &= \int_{\mathcal{S}^{K-1}} \exp(\boldsymbol{\eta}^T \mathbf{x}) d\mu \\ &= \int_0^1 \int_0^{1-x_1} \cdots \int_0^{1-x_1-\cdots-x_{K-2}} \exp\left(\sum_{i=1}^{K-1} \eta_i x_i\right) dx_{K-1} \cdots dx_2 dx_1. \end{aligned} \quad (3)$$

For the innermost integral, we have:

$$\begin{aligned} &\int_0^{1-x_1-\cdots-x_{K-2}} \exp\left(\sum_{i=1}^{K-1} \eta_i x_i\right) dx_{K-1} \\ &= \exp\left(\sum_{i=1}^{K-2} \eta_i x_i\right) \int_0^{1-x_1-\cdots-x_{K-2}} \exp(\eta_{K-1} x_{K-1}) dx_{K-1} \\ &= \exp\left(\sum_{i=1}^{K-2} \eta_i x_i\right) \left[\frac{1}{\eta_{K-1}} \exp(\eta_{K-1} t) \right]_{t=0}^{t=1-x_1-\cdots-x_{K-2}} \\ &= \frac{1}{\eta_{K-1}} \exp\left(\sum_{i=1}^{K-2} \eta_i x_i\right) [\exp(\eta_{K-1}(1-x_1-\cdots-x_{K-2})) - 1] \\ &= \frac{1}{(\eta_{K-1} - \eta_K)} \left[\exp(\eta_{K-1}) \exp\left(\sum_{i=1}^{K-2} (\eta_i - \eta_{K-1}) x_i\right) - \exp\left(\sum_{i=1}^{K-2} \eta_i x_i\right) \right]. \end{aligned} \quad (4)$$

Letting $\eta_i^{(1)} = \eta_i - \eta_{K-1}$ for $i = 1, \dots, K-2$, and $\eta_{K-1}^{(1)} = 0$, by inductive hypothesis we have that:

$$\begin{aligned}
 C_K(\boldsymbol{\eta}^{(1)})^{-1} &= \int_0^1 \int_0^{1-x_1} \cdots \int_0^{1-x_1-\cdots-x_{K-3}} \exp\left(\sum_{i=1}^{K-2} (\eta_i - \eta_{K-1})x_i\right) dx_{K-2} \cdots dx_2 dx_1 \\
 &= (-1)^K \sum_{k=1}^{K-1} \frac{\exp(\eta_k^{(1)})}{\prod_{i \neq k} (\eta_i^{(1)} - \eta_k^{(1)})} \\
 &= (-1)^K \sum_{k=1}^{K-1} \frac{\exp(\eta_i - \eta_{K-1})}{\prod_{i \neq k} (\eta_i - \eta_k)}. \tag{5}
 \end{aligned}$$

Similarly, letting $\eta_i^{(2)} = \eta_i$ for $i = 1, \dots, K-2$, and $\eta_{K-1}^{(2)} = 0$, we have that:

$$\begin{aligned}
 C_K(\boldsymbol{\eta}^{(2)})^{-1} &= \int_0^1 \int_0^{1-x_1} \cdots \int_0^{1-x_1-\cdots-x_{K-3}} \exp\left(\sum_{i=1}^{K-2} \eta_i x_i\right) dx_{K-2} \cdots dx_2 dx_1 \\
 &= (-1)^K \sum_{k=1}^{K-1} \frac{\exp(\eta_k^{(2)})}{\prod_{i \neq k} (\eta_i^{(2)} - \eta_k^{(2)})} \\
 &= (-1)^K \left[\sum_{k=1}^{K-2} \frac{\exp(\eta_k)}{(-\eta_k) \prod_{i \neq k} (\eta_i - \eta_k)} + \frac{1}{\prod_{i=1}^{K-2} \eta_i} \right] \\
 &= (-1)^K \left[\sum_{k=1}^{K-2} \frac{\exp(\eta_k)}{-(\eta_k - \eta_K) \prod_{i \neq k} (\eta_i - \eta_k)} + \frac{\exp(\eta_K)}{\prod_{i=1}^{K-2} (\eta_i - \eta_K)} \right]. \tag{6}
 \end{aligned}$$

Plugging (5) and (6) back into (4), we find:

$$C_K(\boldsymbol{\eta})^{-1} = (-1)^{K+1} \sum_{k=1}^K R_k(\boldsymbol{\eta}) \exp(\eta_k),$$

where the coefficients $R_k(\boldsymbol{\eta})$ gather the terms that multiply each $\exp(\eta_k)$ term. For $k = 1, \dots, K-2$, both (5) and (6) contribute to the coefficient:

$$\begin{aligned}
 R_k(\boldsymbol{\eta}) &= \frac{1}{\eta_{K-1} - \eta_K} \left[-\frac{1}{\prod_{1 \leq i \leq K-1, i \neq k} (\eta_i - \eta_k)} + \frac{1}{\prod_{1 \leq i \leq K, i \neq k, i \neq K-1} (\eta_i - \eta_k)} \right] \\
 &= \frac{1}{\eta_{K-1} - \eta_K} \left[\frac{-\eta_K + \eta_k + \eta_{K-1} - \eta_k}{\prod_{1 \leq i \leq K, i \neq k} (\eta_i - \eta_k)} \right] \\
 &= \frac{1}{\prod_{i \neq k} (\eta_i - \eta_k)}. \tag{7}
 \end{aligned}$$

The $(K-1)$ th coefficient can be computed more directly as it only appears in (5):

$$\begin{aligned}
 R_{K-1}(\boldsymbol{\eta}) &= -\frac{1}{\eta_{K-1} - \eta_K} \frac{1}{\prod_{1 \leq i \leq K-2} (\eta_i - \eta_{K-1})} \\
 &= \frac{1}{\prod_{i \neq K-1} (\eta_i - \eta_{K-1})}, \tag{8}
 \end{aligned}$$

and similarly, the K th coefficient appears only in (6):

$$\begin{aligned}
 R_K(\boldsymbol{\eta}) &= \frac{1}{\eta_{K-1} - \eta_K} \frac{1}{\prod_{1 \leq i \leq K-2} (\eta_i - \eta_{K-1})} \\
 &= \frac{1}{\prod_{i \neq K} (\eta_i - \eta_K)}. \tag{9}
 \end{aligned}$$

This completes the proof. \square

B. Additional properties of the CC distribution

B.1. Mean and covariance

As mentioned in the main manuscript, thanks to exponential family properties, the mean and covariance of the CC can be obtained by differentiating the normalizing constant. For the sake of completeness, we include these results here. If $\mathbf{x} \sim \mathcal{CC}(\boldsymbol{\eta})$, then the mean of \mathbf{x} is given by:

$$\mathbb{E}[x_i] = -\frac{\partial}{\partial \eta_i} \log C(\boldsymbol{\eta}), \quad (10)$$

and the covariance is given by:

$$\text{cov}(x_i, x_j) = -\frac{\partial^2}{\partial \eta_i \partial \eta_j} \log C(\boldsymbol{\eta}). \quad (11)$$

B.2. KL Divergence

The KL divergence between two CC variates can be computed directly from their means:

$$\begin{aligned} KL(p(\mathbf{x}|\boldsymbol{\eta})||p(\mathbf{x}|\tilde{\boldsymbol{\eta}})) &= \mathbb{E}_{p(\mathbf{x}|\boldsymbol{\eta})} \left[\log \frac{p(\mathbf{x}|\boldsymbol{\eta})}{p(\mathbf{x}|\tilde{\boldsymbol{\eta}})} \right] \\ &= \mathbb{E}_{p(\mathbf{x}|\boldsymbol{\eta})} \left[\log C(\boldsymbol{\eta}) - \log C(\tilde{\boldsymbol{\eta}}) + \sum_{i=1}^{K-1} (\eta_i - \tilde{\eta}_i) x_i \right] \\ &= \log C(\boldsymbol{\eta}) - \log C(\tilde{\boldsymbol{\eta}}) + \sum_{i=1}^{K-1} (\eta_i - \tilde{\eta}_i) \mathbb{E}_{p(\mathbf{x}|\boldsymbol{\eta})}[x_i]. \end{aligned} \quad (12)$$

B.3. Moment generating function

The moment generating function of the CC distribution can be written directly in terms of the normalizing constant:

$$\begin{aligned} M_{\mathbf{x}}(\mathbf{t}) &= \mathbb{E}[e^{\mathbf{t}^T \mathbf{x}}] \\ &= \int_{\mathbb{S}^{K-1}} e^{\mathbf{t}^T \mathbf{x}} C(\boldsymbol{\eta}) e^{\boldsymbol{\eta}^T \mathbf{x}} d\mu \\ &= C(\boldsymbol{\eta}) \int_{\mathbb{S}^{K-1}} e^{(\mathbf{t}+\boldsymbol{\eta})^T \mathbf{x}} d\mu \\ &= \frac{C(\boldsymbol{\eta})}{C(\mathbf{t} + \boldsymbol{\eta})}. \end{aligned} \quad (13)$$

The characteristic function can be derived similarly.

B.4. Marginalization

Unlike the Dirichlet, the CC is not preserved under marginalization, even when allowing transformations of the parameter vector. In other words, if $(x_1, \dots, x_{K-1}) \sim \mathcal{CC}(\eta_1, \dots, \eta_{K-1})$, then it is not true that $x_1 \sim \mathcal{CC}(\eta_1)$, nor that $(x_1, \dots, x_{K-2}) \sim \mathcal{CC}(\eta_1, \dots, \eta_{K-2})$. It is not even true that $x_1 \sim \mathcal{CC}(\tilde{\eta}_1)$, nor that $(x_1, \dots, x_{K-2}) \sim \mathcal{CC}(\tilde{\eta}_1, \dots, \tilde{\eta}_{K-1})$, for any $\tilde{\boldsymbol{\eta}}$. This can be seen easily by integrating out the case $K = 3$:

$$\begin{aligned} \int_0^{1-x_1} C(\eta_1, \eta_2) \exp(\eta_1 x_1 + \eta_2 x_2) dx_2 &= C(\eta_1, \eta_2) \exp(\eta_1 x_1) \left[\frac{\exp(\eta_2 t)}{\eta_2} \right]_{t=0}^{t=1-x_1} \\ &= \frac{C(\eta_1, \eta_2) \exp(\eta_2)}{\eta_2} \exp((\eta_1 - \eta_2)x_1) - \frac{C(\eta_1, \eta_2)}{\eta_2} \exp(\eta_1 x_1), \end{aligned} \quad (14)$$

which is not of the form $C(\tilde{\eta}_1) \exp(\tilde{\eta}_1 x_1)$ for any $\tilde{\eta}_1$.

As a direct consequence, we cannot use a stick-breaking construction (Sethuraman, 1994; Paisley et al., 2010) to simulate CC variates from 1-dimensional CB variates, as with the Dirichlet and the Beta distributions.

C. Sampling

In this section, we develop sampling algorithms for the CC distribution and analyze their performance empirically. We also describe how to use our samplers to obtain reparameterization gradients (Kingma & Welling, 2014).

C.1. The ‘naive’ rejection sampler

Given the form of the CC density function, a rejection sampling scheme follows readily by combining independent 1-dimensional CB draws (algorithm 1).

Algorithm 1 Naive sampler

Input: target distribution $\mathcal{CC}(\boldsymbol{\lambda})$.

Output: sample \mathbf{x} drawn from target.

- 1: For $i = 1, \dots, K - 1$, draw $x_i \sim \mathcal{CC}(\lambda_i, \lambda_K)$ independently.
 - 2: If $\sum_{i=1}^{K-1} x_i > 1$, go back to step 1, otherwise return $\mathbf{x} = (x_1, \dots, x_{K-1})$.
-

To see why algorithm 1 achieves the desired distribution, firstly note that by independence, the distribution produced in step 1 is:

$$p_{\text{step1}}(\mathbf{x}) \propto \prod_{i=1}^{K-1} \lambda_i^{x_i} \lambda_K^{1-x_i} \propto \lambda_1^{x_1} \dots \lambda_{K-1}^{x_{K-1}} \lambda_K^{1-x_1-\dots-x_{K-1}}. \quad (15)$$

This is precisely the density we seek, except it is drawn on $[0, 1]^{K-1}$ instead of the simplex. Step 2 rejects all such samples that fall outside the simplex, thus achieving the target distribution.

The obvious shortcoming of this sampling approach is that, even for moderate values of K , the proportion of rejections becomes large. This is particularly troublesome in the balanced case, $\mathbf{x} \sim \mathcal{CC}(1/K, \dots, 1/K)$, which is equivalent to drawing uniformly on $[0, 1]^{K-1}$ and rejecting whenever we fall outside of a simplex of measure $1/(K-1)!$. In other words, we accept with a probability that decays factorially in dimension.

C.1.1. REPARAMETERIZATION

The 1-dimensional CB distribution can be reparameterized using the analytical expression for the inverse CDF, derived by Loaiza-Ganem & Cunningham (2019). In this section we extend the strategy to a multivariate analogue for the CC distribution. The underlying idea is that the rejection step in algorithm 1 only depends on the L_1 norm of the proposal, but not on the parameter. This implies that, once we find an accepted proposal, we can use the inverse CDF reparameterization directly, without requiring a correction term as per the general framework for acceptance-rejection reparameterization gradients (Naesseth et al., 2017).

Our aim is to write $\mathbf{x} = g(\mathbf{u}, \boldsymbol{\lambda})$, where the density of \mathbf{u} does not depend on $\boldsymbol{\lambda}$. To this end, write $F(x|\lambda_i, \lambda_K)$ for the CDF of $x \sim \mathcal{CC}(\lambda_i, \lambda_K)$. Note that this expression will follow readily from an equivalent CB distribution, as $\mathcal{CC}(\lambda_i, \lambda_K) = \mathcal{CB}(\lambda_i/(\lambda_i + \lambda_K))$. For each $i = 1, \dots, K - 1$, applying the inverse CDF component-wise on each of $u_i \stackrel{iid}{\sim} U(0, 1)$ results in $F^{-1}(u_i|\lambda_i, \lambda_K) \sim \mathcal{CC}(\lambda_i, \lambda_K)$. Thus, the vector

$$\mathbf{F}^{-1}(\mathbf{u}|\boldsymbol{\lambda}) := [F^{-1}(u_1|\lambda_1, \lambda_K), \dots, F^{-1}(u_{K-1}|\lambda_{K-1}, \lambda_K)] \quad (16)$$

provides a differentiable reparameterization of the distribution $\mathcal{CC}(\boldsymbol{\lambda})$, provided \mathbf{u} was drawn from the pre-image of the simplex \mathbb{S}^{K-1} under the mapping \mathbf{F}^{-1} , or in other words, provided that $\mathbf{u} \in \mathbf{F}(\mathbb{S}^{K-1})$. The rejection step simply guarantees that we find a sample of uniforms inside this region, but once we have found such a sample, it will lie in the interior of the region with probability 1, and therefore we can differentiate through the transformation as desired:

$$\frac{\partial \mathbf{x}}{\partial \boldsymbol{\lambda}} = \frac{\partial}{\partial \boldsymbol{\lambda}} \mathbf{F}^{-1}(\mathbf{u}|\boldsymbol{\lambda}). \quad (17)$$

We formalize this reparameterization in algorithm 2.

Algorithm 2 Reparameterized rejection sampler

Input: target distribution $\mathcal{CC}(\boldsymbol{\lambda})$.

Output: a sample \mathbf{u} such that $\mathbf{F}^{-1}(\mathbf{u}|\boldsymbol{\lambda}) \sim \mathcal{CC}(\boldsymbol{\lambda})$.

- 1: For $i = 1, \dots, K - 1$, draw $u_i \sim U(0, 1)$ and set $x_i = F^{-1}(x|\lambda_i, \lambda_K)$.
 - 2: If $\sum_{i=1}^K x_i > 1$, return to step 1, otherwise return $\mathbf{u} = (u_1, \dots, u_{K-1})$.
-

C.2. The ordered rejection sampler

An analysis of algorithm 1 reveals two relevant observations. Firstly, the simulation of each $x_j \sim \mathcal{CC}(\lambda_j, \lambda_K)$ in step 1 involves computing the inverse cdf $F^{-1}(\cdot|\lambda_i, \lambda_K)$, which is more expensive than computing the cumulative sum $\sum_{i=1}^j x_i$ of the draws. It therefore pays to recompute the cumulative sums after each draw and go directly to the rejection step as soon as it exceeds 1. Secondly, note that we do not generally expect the components of $\boldsymbol{\lambda}$ to be balanced. Thus, even though simulating each x_i in step 1 requires the same amount of computation, those drawn from smaller values of λ_i are more likely to be close to 0 than those drawn from higher values of λ_i . The dimensions that are more likely to be close to 0 are also less likely to make our cumulative sum exceed the rejection threshold. It therefore also pays to draw the x_i components in order of decreasing λ_i .

These remarks motivate an improved sampling scheme, which we call the ordered rejection sampler (algorithm 3). Empirically, we find that this sampler substantially reduces the rejection rate (see figure 1) as well as the computation time (by not only rejecting less, but also rejecting sooner). However, this sampler performs poorly when $\boldsymbol{\lambda}$ is balanced; such a setting leaves little room for improvement from the re-ordering operation, and the resulting sampler is similar to the naive rejection sampler. This motivates a further sampling scheme that we introduce in the following section, but further improvements to this sampler are left to future work. Lastly, we note that the reparameterization scheme of section C.1.1 can be modified trivially to apply here also.

Algorithm 3 Ordered rejection sampler

Input: target distribution $\mathcal{CC}(\boldsymbol{\lambda})$.

Output: sample \mathbf{x} drawn from target.

- 1: Find the permutation π that orders $\boldsymbol{\lambda}$ from largest to smallest, and let $\tilde{\boldsymbol{\lambda}} = \pi(\boldsymbol{\lambda})$.
 - 2: Set the cumulative sum $c \leftarrow 0$ and $i \leftarrow 2$.
 - 3: **while** $c < 1$ **do**
 - 4: Draw $u_i \sim U(0, 1)$.
 - 5: Set $x_i = F^{-1}(u_i|\lambda_i, \tilde{\lambda}_1)$.
 - 6: Set $c \leftarrow c + x_i$.
 - 7: Set $i \leftarrow i + 1$.
 - 8: **end while**
 - 9: If $c > 1$, go back to step 2.
 - 10: Set $x_1 = 1 - \sum_{i=2}^K x_i$.
 - 11: Return $\mathbf{x} = \pi^{-1}(x_1, \dots, x_K)$.
-

C.3. The permutation sampler

Next, we develop a permutation sampler that performs particularly well for configurations of $\boldsymbol{\lambda}$ that are balanced (those that lead to distributions that are close to uniform). Our key insights here are that the unit cube can be partitioned into simplexes, each of which corresponds to a permutation of its dimensions, and that the CC distribution is, in a sense, ‘invariant’ over these permutations.

C.3.1. PARTITIONING THE CUBE INTO SIMPLEXES

Let $\mathcal{R} = [0, 1]^{K-1}$, the unit cube. For a permutation $\sigma : \{1, 2, \dots, K - 1\} \rightarrow \{1, 2, \dots, K - 1\}$, we denote $\mathcal{S}_\sigma = \{\mathbf{x} \in \mathbb{R}^{K-1} : 0 \leq x_{\sigma(1)} \leq x_{\sigma(2)} \leq \dots \leq x_{\sigma(K-1)} \leq 1\}$. We can then partition (up to intersections of Lebesgue measure zero)

the cube using the $(K - 1)!$ different permutations:

$$\mathcal{R} = \bigcup_{\sigma} \mathcal{S}_{\sigma}, \quad (18)$$

where the union is over all permutations. While our sample space $\text{cl}(\mathbb{S}^{K-1})$, is not equal to \mathcal{S}_{σ} for any σ , we will see in section C.3.2 that sampling from $\text{cl}(\mathbb{S}^{K-1})$ and sampling from \mathcal{S}_{id} are equivalent, where id is the identity permutation. However, as we will see in section C.3.3, sampling from \mathcal{S}_{id} allows to take advantage of the cube partitioning of equation 18, while the same cannot be done for $\text{cl}(\mathbb{S}^{K-1})$.

C.3.2. THE EQUIVALENCE OF SAMPLING OVER ANY SIMPLEX

In this section, we consider varying the support of our CC density from the standard simplex, to other simplexes as well as the unit cube. We denote the support explicitly by writing $\mathbf{x} \sim \mathcal{CC}_{\mathcal{A}}(\boldsymbol{\eta})$ for the density:

$$p_{\mathcal{A}}(\mathbf{x}|\boldsymbol{\eta}) \propto \exp\left(\sum_{i=1}^{K-1} \eta_i x_i\right) \mathbb{1}(\mathbf{x} \in \mathcal{A}) \quad (19)$$

where the subscript \mathcal{A} will typically denote a simplex. Now, letting $\mathbf{x} \sim \mathcal{CC}_{\mathcal{A}}(\boldsymbol{\eta})$ and $\mathbf{y} = Q\mathbf{x}$, where $Q \in \mathbb{R}^{(K-1) \times (K-1)}$ is an invertible matrix, it follows by the change of variable formula that:

$$\begin{aligned} p_{Q(\mathcal{A})}(\mathbf{y}|\boldsymbol{\eta}) &= \frac{1}{|\det(Q)|} p_{\mathcal{A}}(Q^{-1}\mathbf{y}|\boldsymbol{\eta}) \\ &\propto \exp(\boldsymbol{\eta}^{\top} [Q^{-1}\mathbf{y}]) \mathbb{1}(\mathbf{y} \in Q(\mathcal{A})) \\ &= \exp([Q^{-\top}\boldsymbol{\eta}]^{\top} \mathbf{y}) \mathbb{1}(\mathbf{y} \in Q(\mathcal{A})), \end{aligned} \quad (20)$$

where $Q(\mathcal{A}) = \{\mathbf{y} : \mathbf{y} = Q\mathbf{x}, \mathbf{x} \in \mathcal{A}\}$. Thus, we have that $\mathbf{y} \sim \mathcal{CC}_{Q(\mathcal{A})}(\tilde{\boldsymbol{\eta}})$, where $\tilde{\boldsymbol{\eta}} = Q^{-\top}\boldsymbol{\eta}$, so that \mathbf{y} has a new CC distribution on a transformed sample space. Moreover, if Q is a permutation matrix and $\mathcal{A} = \mathcal{S}_{\sigma}$ for some permutation σ , then $Q(\mathcal{A})$ is a ‘permuted’ simplex, and $\tilde{\boldsymbol{\eta}}$ is a rearranged parameter vector, hence the equivalence of sampling over any simplex for the CC.

C.3.3. THE PERMUTATION SAMPLING ALGORITHM

Now, consider a lower triangular matrix of ones:

$$B = \begin{pmatrix} 1 & 0 & 0 & \cdots & 0 \\ 1 & 1 & 0 & \cdots & 0 \\ 1 & 1 & 1 & \cdots & 0 \\ \vdots & \vdots & \vdots & \ddots & \vdots \\ 1 & 1 & 1 & \cdots & 1 \end{pmatrix}. \quad (21)$$

Note that $\mathcal{S}_{id} = B(\text{cl}(\mathbb{S}^{K-1}))$, so that sampling from $\mathcal{CC}_{\text{cl}(\mathbb{S}^{K-1})}(\boldsymbol{\eta})$ is equivalent to sampling from $\mathcal{CC}_{\mathcal{S}_{id}}(\tilde{\boldsymbol{\eta}})$ and transforming the result with B^{-1} , where $\tilde{\boldsymbol{\eta}} = B^{-\top}\boldsymbol{\eta}$. We present a rejection sampling scheme to draw from $\mathcal{CC}_{\mathcal{S}_{id}}(\tilde{\boldsymbol{\eta}})$ in algorithm 4. As with the naive sampler, our proposal is drawn on the whole unit cube from independent 1-dimensional CB variates, but the advantage here is that we do not have to directly reject the sample if it fell outside of the desired simplex \mathcal{S}_{id} , but rather we can transform it onto that simplex and then accept it with an appropriate probability (which we can compute easily using the invariance property). Here, the acceptance probability depends on which simplex the proposal fell into, and is given by:

$$\alpha(\mathbf{y}', \boldsymbol{\eta}^{(1)}, \boldsymbol{\eta}^{(2)}) = \frac{p_{\mathcal{S}_{id}}(\mathbf{y}'|\boldsymbol{\eta}^{(1)})}{\kappa(\boldsymbol{\eta}^{(1)}, \boldsymbol{\eta}^{(2)}) p_{\mathcal{S}_{id}}(\mathbf{y}'|\boldsymbol{\eta}^{(2)})}, \quad (22)$$

where $\kappa(\boldsymbol{\eta}^{(1)}, \boldsymbol{\eta}^{(2)})$ is the rejection sampling constant, which in this case is equal to:

$$\kappa(\boldsymbol{\eta}^{(1)}, \boldsymbol{\eta}^{(2)}) = \max_{\mathbf{y} \in \mathcal{S}_{id}} \frac{p_{\mathcal{S}_{id}}(\mathbf{y}|\boldsymbol{\eta}^{(1)})}{p_{\mathcal{S}_{id}}(\mathbf{y}|\boldsymbol{\eta}^{(2)})}. \quad (23)$$

Algorithm 4 Permutation sampler

Input: target distribution $\mathcal{CC}_{\mathcal{S}_{id}}(\tilde{\boldsymbol{\eta}})$.

Output: sample \mathbf{y} drawn from target.

- 1: Sample $\mathbf{y} \sim \mathcal{CC}_{\mathcal{R}}(\tilde{\boldsymbol{\eta}})$ (again, this is straightforward to do by sampling each coordinate independently).
 - 2: Sort the elements of \mathbf{y} . In other words, find a permutation σ such that $\sigma(\mathbf{y}) \in \mathcal{S}_{id}$. Let P be the corresponding permutation matrix and $\mathbf{y}' = P\mathbf{y}$.
 - 3: Accept \mathbf{y}' with probability $\alpha(\mathbf{y}', \tilde{\boldsymbol{\eta}}, P^{-\top} \tilde{\boldsymbol{\eta}})$. Otherwise, go back to step 1.
-

The algorithm samples correctly from $\mathcal{CC}_{\mathcal{S}_{id}}(\tilde{\boldsymbol{\eta}})$, because \mathbf{y} can be thought of as a sample from $p_{\mathcal{R}}(\mathbf{y}|\boldsymbol{\eta}, \mathbf{y} \in \mathcal{S}_{\sigma}) = p_{\mathcal{S}_{\sigma}}(\mathbf{y}|\boldsymbol{\eta})$, which we then transform with P to obtain a distribution on \mathcal{S}_{id} . If we use this distribution as a proposal distribution for a rejection sampling algorithm, we recover precisely the acceptance probability of equation 22. Intuitively, if our sample \mathbf{x} does not fall on the desired simplex \mathcal{S}_{id} , we move around the simplex in which it fell (along with \mathbf{x} itself) so that it matches the desired simplex, and then do rejection sampling.

We conclude this subsection with two short notes on the optimization problem of equation 23. The first one is that when $\boldsymbol{\eta}^{(2)} = Q^{-\top} \boldsymbol{\eta}^{(1)}$ where $|\det(Q)| = 1$, then the normalizing constants cancel out, which is the case in our algorithm since $|\det(P)| = 1$. The second is that, by taking logs, the optimization problem can be transformed into a linear problem subject to linear inequality constraints, meaning that the solution must be achieved at a vertex. Since there are K vertices, namely $\mathbf{0}$, \mathbf{e}_{K-1} , $\mathbf{e}_{K-1} + \mathbf{e}_{K-2}, \dots, \sum_{i=1}^{K-1} \mathbf{e}_i$, we can solve the problem by simply checking each of these vertices.

C.4. Performance

While the ordered rejection sampler can never have a worse rejection rate than its naive counterpart, the comparison with the permutation sampler depends on the shape of the target distribution, as discussed. The perfectly balanced case $\boldsymbol{\lambda} = (1/K, \dots, 1/K)$ results in the worst possible rejection rate for the ordered rejection sampler (we accept with probability $1/(K-1)!$), but also the best possible rejection rate for the permutation sampler (this is the uniform case so $\alpha(\mathbf{y}', \boldsymbol{\eta}^{(1)}, \boldsymbol{\eta}^{(2)}) = 1$). On the other end of the spectrum, in the totally unbalanced case where one element of $\boldsymbol{\lambda}$ holds all the weight and the others are close to zero, the ordered rejection sampler achieves an acceptance rate close to 1, whereas it is much smaller for the permutation sampler (see section C.4.3). In this sense, our samplers are complementary, and an optimal sampling algorithm could involve combining accept/reject steps from both methods. We study the performance of our samplers empirically, by comparing the distribution of the rejection rates under a sparsity-inducing prior $\boldsymbol{\lambda} \sim \text{Dirichlet}(1/K, \dots, 1/K)$. Indeed, the ordered rejection sampler tends to considerably outperform the permutation sampler (see figure 1), as well as (trivially) the naive sampler.

Now, it may come as a surprise that the permutation sampler does not necessarily outperform the naive sampler. After all, the naive sampler only accepts samples that fell directly into the desired simplex, whereas the permutation sampler has the additional possibility of accepting a sample that fell outside of \mathcal{S}_{id} after applying a suitable permutation. However, this intuition breaks down once we realize that the proposal distributions from the two methods are not equivalent. We make this precise in the following sections.

C.4.1. REJECTION RATE - NAIVE SAMPLER

Suppose we seek $\mathbf{x} \sim \mathcal{CC}_{\text{cl}(\mathbb{S}^{K-1})}(\boldsymbol{\eta})$. The naive rejection sampler proposes $\mathbf{x} \sim \mathcal{CC}_{\mathcal{R}}(\boldsymbol{\eta})$, and accepts if $\mathbf{x} \in \mathbb{S}^{K-1}$. The proposal density is equal to (we know the normalizing constant as we have the product of independent CBs):

$$p_{\mathcal{R}}(\mathbf{x}|\boldsymbol{\eta}) = \prod_{i=1}^{K-1} \frac{\eta_i}{e^{\eta_i} - 1} e^{\eta_i x_i}. \quad (24)$$

Therefore, the probability of acceptance is:

$$P(\mathcal{CC}_{\mathcal{R}}(\boldsymbol{\eta}) \in \mathbb{S}^{K-1}) = \int_{\mathbb{S}^{K-1}} \prod_{i=1}^{K-1} \frac{\eta_i}{e^{\eta_i} - 1} e^{\eta_i x_i} d\mu. \quad (25)$$

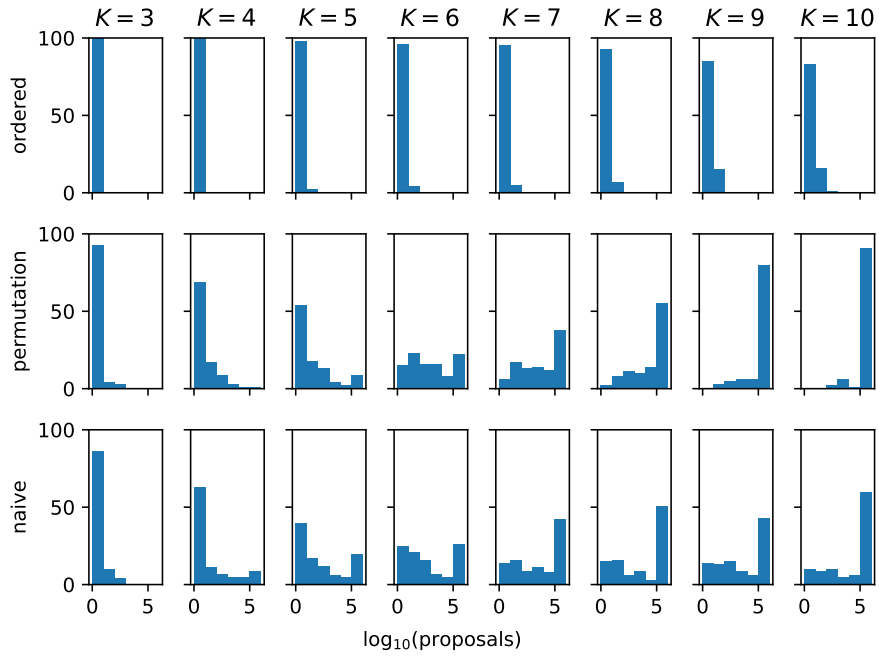


Figure 1. Shows the performance of 3 sampling algorithms across different dimensions K . Each histogram shows the distribution, over 100 trials, of the number of proposals required for 1 acceptance, on the log scale (base 10). The distributions are not exponential, since each of the 100 trials is sampled from a different $CC(\boldsymbol{\lambda})$ distribution, where the parameter follows $\boldsymbol{\lambda} \stackrel{iid}{\sim} \text{Dirichlet}(1/K, \dots, 1/K)$. Due to computational constraints, the number of proposals in each trial is right-censored, hence the large bars at the right end of the histograms.

We can apply the transformation B to rewrite this as:

$$P(B(\mathcal{CC}_{\mathcal{R}}(\boldsymbol{\eta})) \in B(\mathbb{S}^{K-1})) = P(\mathcal{CC}_{B(\mathcal{R})}(B^{-\top}\boldsymbol{\eta}) \in \mathcal{S}_{id}) = \int_{\mathcal{S}_{id}} \prod_{i=1}^{K-1} \frac{\eta_i}{e^{\eta_i} - 1} e^{\tilde{\eta}_i x_i} d\mu, \quad (26)$$

where we have used the fact that $|\det(B)| = 1$ so that the normalizing constant remains unchanged. Thus, the probability of acceptance of the naive sampler is equal to:

$$P(\text{accept}) = \left(\prod_{i=1}^{K-1} \frac{\eta_i}{e^{\eta_i} - 1} \right) \cdot \int_{\mathcal{S}_{id}} e^{\tilde{\boldsymbol{\eta}}^\top \mathbf{x}} d\mu. \quad (27)$$

C.4.2. REJECTION RATE - PERMUTATION SAMPLER

In the case of the permutation sampler, the acceptance rate is harder to compute. However, one can easily obtain a lower bound by considering only the samples that fall directly into our target simplex (in this case, \mathcal{S}_{id}). In this case, the proposal distribution is:

$$p_{\mathcal{R}}(\mathbf{x}|\tilde{\boldsymbol{\eta}}) = \prod_{i=1}^{K-1} \frac{\tilde{\eta}_i}{e^{\tilde{\eta}_i} - 1} e^{\tilde{\eta}_i x_i}. \quad (28)$$

If the resulting sample falls in \mathcal{S}_{id} , we accept the sample and map it back to $\text{cl}(\mathbb{S}^{K-1})$. Thus, the acceptance rate has the lower bound

$$P(\text{accept}) \geq \left(\prod_{i=1}^{K-1} \frac{\tilde{\eta}_i}{e^{\tilde{\eta}_i} - 1} \right) \cdot \int_{\mathcal{S}_{id}} e^{\tilde{\boldsymbol{\eta}}^\top \mathbf{x}} d\mu. \quad (29)$$

Note that, while this lower bound has the same integral term as the naive rejection sampler, it is multiplied by a different normalizing constant. In particular, there are configurations of $\boldsymbol{\eta}$ that can lead to much worse normalizing constants for the permutation sampler than for the naive rejection sampler, resulting in a worse acceptance rate overall.

C.4.3. EXAMPLE

We give an example of a configuration of $\boldsymbol{\eta}$ such that the acceptance rate of the naive sampler is better than that of the permutation sampler. Consider the case $(\eta_1, \dots, \eta_{K-1}) = (-M, \dots, -M)$, where M is a large positive number. Note that this example is far from the uniform case $\boldsymbol{\lambda} = (1/K, \dots, 1/K)$. In fact, in this case, after transforming with B , we obtain $\tilde{\eta}_{K-1} = -M$, and $\tilde{\eta}_{K-2} = \dots = \tilde{\eta}_1 = 0$. Thus, when we sample a proposal $\mathbf{y} \sim \mathcal{CC}_{\mathcal{R}}(\tilde{\boldsymbol{\eta}})$, typically y_{K-1} will be small relative to y_1, \dots, y_{K-2} , which will be ordered at random. This means the sorting step of our permutation sampler will likely map y_{K-1} to y'_1 , as well as sorting the remaining entries $y'_2 < \dots < y'_{K-1}$. In other words, P maps the $(K-1)^{th}$ entry to the 1st entry, and one of the first $K-2$ entries to the $(K-1)^{th}$ entry (whichever of these happens to sample the largest value). The resulting distributions $p_{\mathcal{S}_{id}}(\cdot|\tilde{\boldsymbol{\eta}})$ and $p_{\mathcal{S}_{id}}(\cdot|P^{-\top}\tilde{\boldsymbol{\eta}})$ are similar, with the key difference that the former puts the negative $\tilde{\boldsymbol{\eta}}$ coefficient (namely $\tilde{\eta}_{K-1} = -M$) in the last position (the largest component of \mathbf{y}), while the latter puts it into some other position determined by σ^{-1} , i.e. the right-most column of P or equivalently, the bottom row of P^{-1} . In this setting, it follows that κ will be equal to 1, and the ratio $p_{\mathcal{S}_{id}}(\mathbf{y}'|\tilde{\boldsymbol{\eta}})/p_{\mathcal{S}_{id}}(\mathbf{y}'|P^{-\top}\tilde{\boldsymbol{\eta}})$ will be small. Thus, our rejection sampling ratio is typically small and we are likely to reject our proposal. The ratio will be close to 1 only in the event that the proposed value x_{K-1} is large relative to the other components x_1, \dots, x_{K-2} , which rarely happens as x_{K-1} is sampled from a univariate CC with much smaller coefficient. Note further, that $\tilde{\boldsymbol{\eta}}$ cannot be re-shuffled in this case, as this would lead to a target distribution on a simplex other than \mathcal{S}_{id} (we can only shuffle $\boldsymbol{\eta}$ prior to applying B , which in this case leaves $\boldsymbol{\eta}$ unchanged). We conclude that we cannot achieve a uniformly better rejection rate through the permutation sampler, relative to the naive method.

References

Gamerman, D. and Lopes, H. F. *Markov chain Monte Carlo: stochastic simulation for Bayesian inference*. Chapman and Hall/CRC, 2006.

- Jang, E., Gu, S., and Poole, B. Categorical reparameterization with gumbel-softmax. *arXiv preprint arXiv:1611.01144*, 2016.
- Kingma, D. P. and Welling, M. Auto-encoding variational bayes. In *2nd International Conference on Learning Representations, ICLR 2014, Banff, AB, Canada, April 14-16, 2014, Conference Track Proceedings*, 2014.
- Loaiza-Ganem, G. and Cunningham, J. P. The continuous bernoulli: fixing a pervasive error in variational autoencoders. In *Advances in Neural Information Processing Systems*, pp. 13266–13276, 2019.
- Maddison, C. J., Mnih, A., and Teh, Y. W. The concrete distribution: A continuous relaxation of discrete random variables. *arXiv preprint arXiv:1611.00712*, 2016.
- Naesseth, C. A., Ruiz, F. J. R., Linderman, S. W., and Blei, D. M. Reparameterization gradients through acceptance-rejection sampling algorithms. In *International Conference on Artificial Intelligence and Statistics*, pp. 489–498, 2017.
- Paisley, J. W., Zaas, A. K., Woods, C. W., Ginsburg, G. S., and Carin, L. A stick-breaking construction of the beta process. In *Proceedings of the 27th International Conference on Machine Learning (ICML-10)*, pp. 847–854, 2010.
- Sethuraman, J. A constructive definition of dirichlet priors. *Statistica sinica*, pp. 639–650, 1994.
- Stirn, A., Jebara, T., and Knowles, D. A. A new distribution on the simplex with auto-encoding applications. *arXiv preprint arXiv:1905.12052*, 2019.